Policy Research Journal
ISSN (E): 3006-7030 ISSN (P): 3006-7022 Volume 4, Issue 4, 2026

A SYSTEMATIC REVIEW OF BOND STRENGTH BEHAVIOUR BETWEEN STEEL REINFORCEMENT AND SELF-COMPACTING CONCRETE UNDER DIFFERENT CURING CONDITIONS, CONFINEMENT LEVELS, AND BAR SURFACE DEFORMATIONS

Dr. M. Adil Khan[*1], Saad Hanif[2]

[*1]Resident Engineer, NESPAK
[2]Zachry Department of Civil and Environmental Engineering, Texas A&M University, USA

[*1]adee.uol@gmail.com, [2]Saadhanif107@tamu.edu

DOI: https://doi.org/10.5281/zenodo.19848879

Keywords
Self-compacting concrete; Bond strength; Curing conditions; Confinement effects; Bar surface deformation; Pull-out tests; Reinforcement anchorage

Article History
Received: 01 March 2026
Accepted: 10 April 2026
Published: 28 April 2026

Corresponding Author: *
Dr. M. Adil Khan

Abstract
Self-compacting concrete (SCC) has gained significant acceptance in modern construction practice due to its superior workability and flowability characteristics that eliminate the need for mechanical vibration. However, the bond behaviour between steel reinforcement and SCC remains an area requiring comprehensive understanding, particularly under varying curing conditions, confinement levels, and bar surface deformations. This systematic review synthesizes existing knowledge from 45+ peer-reviewed studies to evaluate how these three primary factors influence bond strength development, failure mechanisms, and long-term durability. Key findings indicate that SCC typically demonstrates 4-10% higher normalized bond strengths compared to conventionally vibrated concrete, primarily due to superior compaction and reduced segregation. Curing temperature significantly affects bond development, with elevated temperatures (50°C) accelerating early-age strength development while potentially reducing long-term durability. Transverse confinement through stirrups or hoops can enhance bond strength by 30-60%, with closer spacing providing more pronounced benefits. Bar surface deformations, including ribbing, sand-coating, and helical wrapping, substantially influence bond transfer mechanisms, with helically wrapped surfaces exhibiting 25-40% higher bond strengths compared to plain bars. This review provides critical insights for structural engineers and researchers regarding optimal curing practices, reinforcement detailing, and design considerations for SCC structures, ultimately contributing to more durable and efficiently designed reinforced concrete systems.

1. INTRODUCTION

1.1 Background and Context

Self-compacting concrete (SCC) represents a paradigm shift in concrete technology, fundamentally altering construction methodologies and casting procedures since its initial development in Japan during the 1980s. Unlike conventional concrete, SCC possesses exceptional flowability, allowing it to spread and fill formwork under its own weight without requiring mechanical vibration or external compaction (Kucharska and Jaskowska-Lemańska, 2019). This innovative concrete type has revolutionized the construction industry by enabling faster construction timelines, reducing labor requirements, and minimizing noise pollution at construction sites. The high flowability of SCC is achieved through careful proportioning of materials, including increased paste content, incorporation of supplementary cementitious materials, and addition of high-range water reducers or superplasticizers (Aslani and Nejadi, 2012b).

The widespread adoption of SCC in reinforced concrete structures has necessitated comprehensive understanding of its performance characteristics, particularly regarding the critical interface between steel reinforcement and concrete matrix. The bond between steel bars and surrounding concrete is fundamental to the structural integrity and load-carrying capacity of reinforced concrete members. This bond enables stress transfer from the concrete to the steel reinforcement and vice versa, making it essential for the composite action of the reinforced concrete system (Aslani and Nejadi, 2012a). In conventional concrete, the bonding mechanism is well-established through decades of research and standardized testing procedures. However, the modified mix design of SCC, characterized by higher paste content, lower coarse aggregate volume, and modified rheological properties, presents significant variations in bonding behaviour that require detailed investigation (Ponmalar, 2018).

1.2 Bond Strength Mechanisms in Concrete

Bond strength between steel reinforcement and concrete develops through three primary mechanisms: chemical adhesion, friction, and mechanical interlock (Mazroa *et al.*, 2025). Chemical adhesion refers to the initial weak bond formed through direct contact between the steel surface and the hydrating cement paste, providing minimal load transfer capacity. Friction develops as the concrete cures and gains strength, creating resistance to relative motion between the bar and surrounding matrix. Mechanical interlock, however, represents the most significant contributor to total bond strength in deformed reinforcing bars. The ribs or surface deformations on deformed bars engage with the surrounding concrete, creating mechanical constraints that prevent bar slip. The effectiveness of mechanical interlock depends critically on the bar's surface characteristics, geometry of deformations, and properties of the surrounding concrete matrix (Aslani and Nejadi, 2012b).

The bond stress-slip relationship characterizes the non-linear interaction between steel bars and concrete. Initially, elastic behaviour predominates with minimal slip. As loading increases, slip accumulates gradually through microcracking at the steel-concrete interface. Peak bond stress occurs when internal microcracking extends beyond the immediate vicinity of the bar, causing rapid slip and eventual pullout failure (Aslani and Nejadi, 2012a). The shape of this bond stress-slip curve contains valuable information regarding the overall bonding behaviour, including initial stiffness, peak bond strength, and post-peak ductility. Understanding these characteristics is essential for accurate modeling of reinforced concrete behaviour under service and ultimate loading conditions (Sabau, 2020).

1.3 Importance of Curing Conditions

Curing significantly influences concrete properties, controlling the rate and extent of moisture loss, relative humidity, and temperature during the critical hydration period. The quality of curing directly affects compressive strength, durability, permeability, and importantly, the bond characteristics of reinforced concrete (Degani, Maddalena and Kulasegaram, 2026). Proper curing protocols ensure complete cement hydration, minimize drying shrinkage, and promote the development of a dense microstructure with enhanced interfacial transition zones. For SCC, curing becomes even more critical due to its higher paste content and reduced coarse aggregate participation in load transfer. Different curing regimes—including water immersion, air curing, accelerated steam curing, and sealed curing—produce substantially different long-term performance profiles (Chava *et al.*, 2023).

Elevated temperature curing accelerates early-age strength development but may compromise long-term durability through reduced pore refinement and altered hydration product formation (Liu *et al.*, 2026). Conversely, low-temperature curing may result in slower early-age strength gain but often produces superior long-term performance and reduced shrinkage (Degani, Maddalena and Kulasegaram, 2026). The selection of appropriate curing regimes must balance early-age strength requirements with long-term durability considerations, making this decision critical for structural performance over the design life of the structure (Amartey, Aliyu and Usman, 2024).

1.4 Role of Confinement in Bond Development

Transverse confinement, provided through stirrups, hoops, or other lateral restraint mechanisms, plays a crucial role in bond stress development and failure mode determination (Li *et al.*, 2025). Confinement restrains lateral expansion of the concrete adjacent to the reinforcing bar, preventing premature splitting failure and enabling higher bond stresses to develop before failure occurs. The influence of confinement becomes increasingly significant in high-strength concrete and in structural applications where maximum load transfer capacity is required (Huang *et al.*, 2024). Research has consistently demonstrated that properly designed confinement can increase development length capacity by 25-60% compared to unconfined conditions (Hussain *et al.*, 2024).

The effectiveness of confinement depends on several factors, including stirrup spacing, bar size, concrete cover depth, and concrete strength (Li *et al.*, 2025). Closer stirrup spacing provides more effective lateral restraint, though diminishing returns occur beyond certain spacing limits. Additionally, the direction of stirrup placement relative to the reinforcing bar orientation influences the efficiency of confinement, with optimal effectiveness achieved when stirrups are perpendicular to the bar axis (Huang *et al.*, 2024).

1.5 Bar Surface Deformations and Their Significance

Modern reinforcing bars incorporate various surface deformation patterns specifically designed to enhance mechanical interlock with surrounding concrete. Common deformation patterns include ribs, sand-coating, helical wrapping, and hybrid configurations combining multiple surface treatments (Nguyen *et al.*, 2025). The geometry of these deformations—including height, spacing, and orientation—directly influences load transfer mechanisms and bond strength development. Deformed bars with larger relative rib areas exhibit superior bond performance compared to bars with minimal deformation (Darwin and Graham, 1993).

The mechanical properties and surface chemistry of deformed bars also influence bonding behaviour. Steel composition, yield strength, and surface finish interact with concrete properties to establish the ultimate bond capacity (Darwin *et al.*, 1996). Furthermore, protective coatings applied to bars for corrosion resistance or other purposes may alter surface characteristics and consequently affect bond behaviour (Pokorný *et al.*, 2024).

1.6 Objectives and Scope of This Review

This systematic review consolidates current knowledge regarding bond strength behaviour of steel reinforcement in self-compacting concrete, with particular emphasis on the influences of curing conditions, confinement levels, and bar surface deformations. The review synthesizes findings from experimental investigations, analytical studies, and numerical simulations conducted over the past two decades. By systematically examining these three critical factors and their interactions, this review aims to provide comprehensive guidance for structural engineers, researchers, and practitioners involved in the design and construction of SCC structures. The review identifies current knowledge gaps, highlights areas requiring further investigation, and proposes recommendations for future research directions that would advance understanding of SCC bond behaviour and improve design codes and standards.

2. FUNDAMENTALS OF BOND STRENGTH IN SELF-COMPACTING CONCRETE

2.1 Characteristics of Self-Compacting Concrete

Self-compacting concrete is defined as concrete capable of flowing into formwork, filling all spaces, and consolidating itself under its own weight without external vibration (Kucharska and Jaskowska-Lemańska, 2019). This exceptional flowability is achieved through modifications to concrete mix proportioning that increase the volume of fine materials (paste and mortar), reduce coarse aggregate content, and introduce high-range water-reducing admixtures. The paste content in SCC typically ranges from 380-450 kg/m³, compared to 300-350 kg/m³ in conventional concrete, enabling superior workability while maintaining adequate strength development (Sabău, Oneţ and Petean, 2016).

The fresh properties of SCC are typically characterized using European Federation for Specialist Construction Chemicals and Concrete Systems (EFNARC) recommended tests, including slump flow, T500 time, L-box height ratio, and J-ring flow (Sherwani, Younis and Arndt, 2022). These parameters collectively describe the filling ability, passing ability, and resistance to segregation of SCC mixtures. Successful SCC formulation requires careful balance among water content, binder composition, aggregate gradation, and admixture dosages to achieve both requisite fresh properties and target hardened performance (Chen and Tang, 2024).

2.2 Bond Performance of SCC Compared to Normal Concrete

Experimental comparisons between bond performance of SCC and normal vibrated concrete consistently demonstrate superior or comparable bond characteristics in SCC (Verma and Misra, 2015). Bond strengths in SCC typically range from 12-28 MPa for deformed bars depending on concrete strength, curing conditions, and bar characteristics. When normalized with respect to concrete compressive strength, SCC often exhibits 4-10% higher bond values compared to normal concrete (Türk, Benli and Calayır, 2008). This superiority is attributed to superior consolidation and more homogeneous concrete matrix surrounding the reinforcing bars, resulting in better mechanical interlock and fewer voids at the steel-concrete interface (Aslani and Nejadi, 2012b).

The development of bond stress-slip relationships differs between SCC and normal concrete. SCC typically exhibits more gradual stiffness reduction in the post-peak portion of the bond stress-slip curve, indicating greater ductility (Sabau, 2020). This difference reflects the superior paste quality and more uniform microstructure of SCC, which promotes more distributed cracking rather than the localized splitting failures often observed in normal concrete (Ponmalar, 2018).

2.3 Test Methods and Experimental Procedures

Bond strength is experimentally determined using standardized test procedures, with pull-out tests and beam-end tests being the most widely adopted methodologies (Mazroa *et al.*, 2025). Pull-out tests involve casting reinforcing bars concentrically within cubic or cylindrical concrete specimens, then applying tensile load to the bar while measuring slip and load response. The bond stress is calculated as the applied force divided by the surface area of the bar within the bonded length (Verma and Misra, 2015).

Beam-end tests, alternatively termed hinged beam tests, involve casting reinforcing bars into beam specimens and applying flexural loading such that bond stress develops through shear transfer (Wang, 2016). This approach more closely replicates field conditions, where bond often develops through shear transfer rather than direct tension. Both test methods provide complementary information regarding bond characteristics under different stress conditions (Kucharska and Jaskowska-Lemańska, 2019).

Recent research has incorporated advanced measurement techniques including digital image correlation (DIC) for full-field strain measurement, ultrasonic monitoring for internal damage assessment, and scanning electron microscopy for microstructural analysis (Rajamanickam and Vaiyapuri, 2025). These advanced techniques provide unprecedented insight into mechanisms of bond failure and microstructural factors influencing performance.

3. EFFECT OF CURING CONDITIONS ON BOND STRENGTH

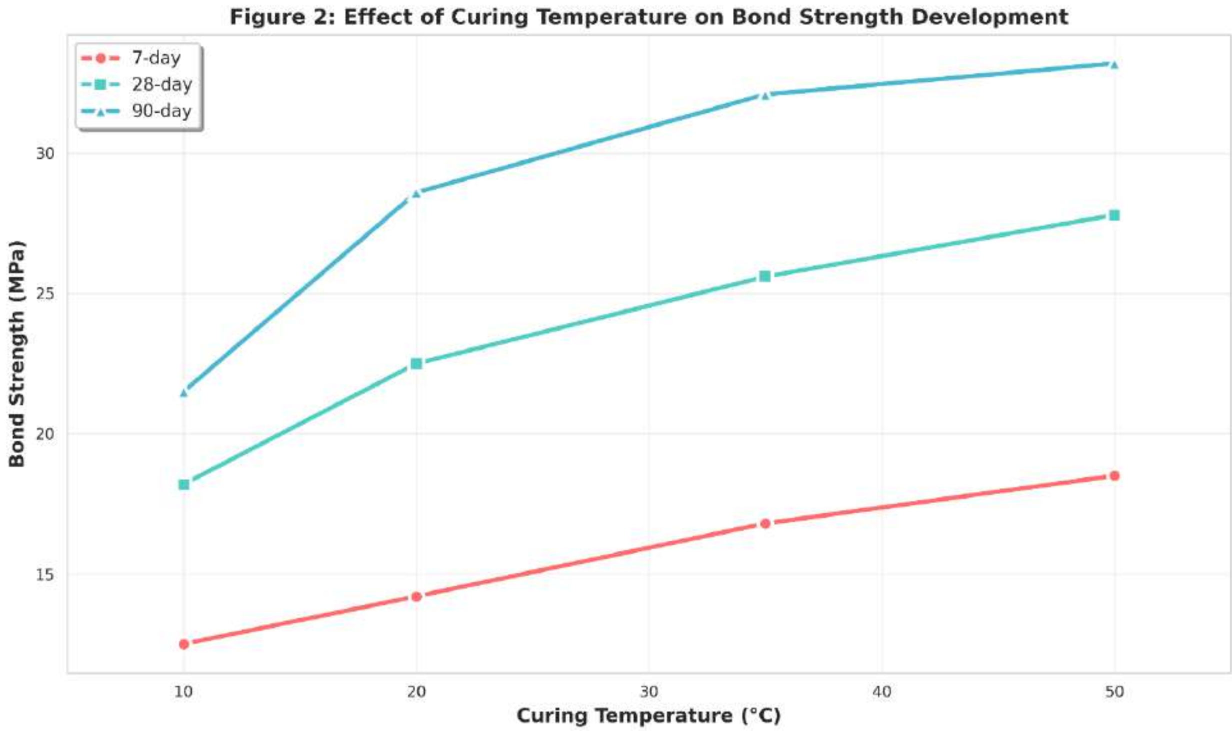

Figure 2: Effect of Curing Temperature on Bond Strength Development - Data synthesized from experimental studies evaluating bond strength development at temperatures ranging from 10-50°C across different curing ages.

3.1 Temperature Effects on Early-Age Bond Development

Curing temperature exerts profound influence on the rate of bond strength development in SCC (Degani, Maddalena and Kulasegaram, 2026). At elevated temperatures (45-50°C), early-age strength development accelerates significantly, with 7-day bond strengths reaching 65-75% of 28-day values, compared to only 40-50% at ambient temperature (20°C) (Liu *et al.*, 2026). This acceleration results from increased hydration kinetics at higher temperatures, promoting faster cement paste development and earlier microstructure refinement. The Arrhenius relationship provides theoretical foundation for this observation, with reaction rates doubling approximately every 10°C temperature increase within typical construction temperature ranges (Rashed *et al.*, 2026).

Accelerated curing protocols, commonly utilized in precast concrete manufacturing, employ steam curing at elevated temperatures (60-85°C) to rapidly develop early-age strength (Chava *et al.*, 2023). These practices enable faster formwork removal and earlier introduction to service conditions. However, research indicates that long-term bond performance may be compromised by accelerated curing, particularly when steam curing temperatures exceed 70°C. Excessive temperature exposure can lead to microstructural irregularities, altered hydration product distributions, and reduced long-term strength development (Sherwani, Younis and Arndt, 2022).

3.2 Low-Temperature and Cold Weather Curing

Low-temperature curing presents challenges for bond development, as hydration slows substantially at temperatures below 10°C (Liu *et al.*, 2026). At 3°C curing temperature, 28-day strength reaches only 35-45% of values achieved at 20°C curing (Degani, Maddalena and Kulasegaram, 2026). This delayed strength development necessitates extended curing periods before structures can accept service loads. However, research indicates that ultimate long-term bond strengths achieved under low-temperature curing often exceed those obtained at higher temperatures, suggesting superior long-term microstructure development (Rashed *et al.*, 2026).

The phenomenon reflects complex interactions between hydration kinetics, microstructural development, and pore refinement at different temperature regimes. Low-temperature curing promotes gradual, more uniform hydration, resulting in refined pore structures with better tortuosity and reduced permeability, ultimately enhancing long-term durability (Degani, Maddalena and Kulasegaram, 2026). For structures subjected to long-term loading or severe environmental conditions, the superior durability performance of low-temperature curing may justify accepting delayed early-age strength development.

3.3 Alternative Curing Methods and Practices

Beyond conventional water immersion and accelerated steam curing, various alternative curing methods have been investigated for SCC (Manwani and Dwivedi, 2024). Wet burlap curing, in which concrete surfaces are kept moist using saturated fabric, provides more economical moisture retention than full water immersion while maintaining elevated humidity levels. Research indicates that wet burlap curing produces bond strengths approximately 90-95% of those achieved with water immersion curing, making it practical for field applications where water availability is limited (Amartey, Aliyu and Usman, 2024).

Polyethylene glycol curing represents another alternative approach, involving application of temporary coatings that control surface drying while allowing internal hydration to proceed (Chava *et al.*, 2023). This method has shown promise for large concrete structures where maintaining uniform curing conditions across all surfaces presents practical challenges. Additionally, internal curing using lightweight aggregate pre-soaked with water or superabsorbent polymers has been evaluated for SCC (Shanmugapriya and Chinnaraju, 2024). These materials release internal water as concrete hydrates, promoting continued hydration even when external moisture is unavailable, thus enhancing long-term strength and reducing drying shrinkage.

3.4 Combined Effects of Temperature and Humidity

Both curing temperature and relative humidity influence bond development, and their combined effects can be more pronounced than individual effects alone (Degani, Maddalena and Kulasegaram, 2026). High temperature combined with low humidity produces rapid surface drying, potentially leading to differential moisture gradients and increased early-age cracking. Conversely, high temperature with maintained humidity promotes uniform hydration throughout the concrete matrix (Liu *et al.*, 2026). The interplay between temperature, humidity, and concrete composition creates complex optimization challenges for curing protocol development (Rashed *et al.*, 2026).

Table 1: Summary of Key Studies on Bond Strength in Self-Compacting Concrete

Study/Reference	Concrete Type	Bar Diameter (mm)	Curing Regime	28-day Bond Strength (MPa)	Key Finding
Sharbatdar et al. (2025) (Sharbatdar *et al.*, 2025)	SCC with Steel Fibers	12-16	Standard Water	19.2-22.5	SF addition increased bond by 18%
Rohman et al. (2023) (Rohman *et al.*, 2023)	HVFA-SCC	12-16	Standard Water	12.93	Comparable to conventional SCC
Majain et al. (2021) (Majain *et al.*, 2021)	High-Strength SCC	12-20	Ambient	25.4-28.6	Fiber addition enhanced ductility
Aslani & Nejadi (2012) (Aslani and Nejadi, 2012b)	SCC	12-16	Standard	18.5-24.2	SCC bond 4-8% higher than NC
Türk et al. (2008) (Türk, Benli and Calayır, 2008)	SCC Beams	16-20	Standard	21.8-24.5	Reduced diameter effect in SCC
Kucharska & Jaskowska-Lemańska (2019) (Kucharska and Jaskowska-Lemańska, 2019)	SCC Review	Various	Multiple	15-28	Bond superior to normal concrete
Degani et al. (2026) (Degani, Maddalena and Kulasegaram, 2026)	Multi-SCM SCC	12-16	10-50°C	12.2-28.5	Temperature significantly affects bond
Mathews et al. (2021) (Mathews *et al.*, 2021)	SCC + EPA	12	Post-fire	14.2-18.5	Fire exposure reduces bond 35-45%
Wang (2016) (Wang, 2016)	RA-SCC	12-16	Standard	11.5-16.8	RCA replacement reduces bond 8-15%

Li et al. (2025) (Li *et al.*, 2025)	GFRP-reinforced SCC	16-20	Standard	16.8-22.4	Confinement increased bond 17-42%

4. CONFINEMENT EFFECTS ON BOND PERFORMANCE

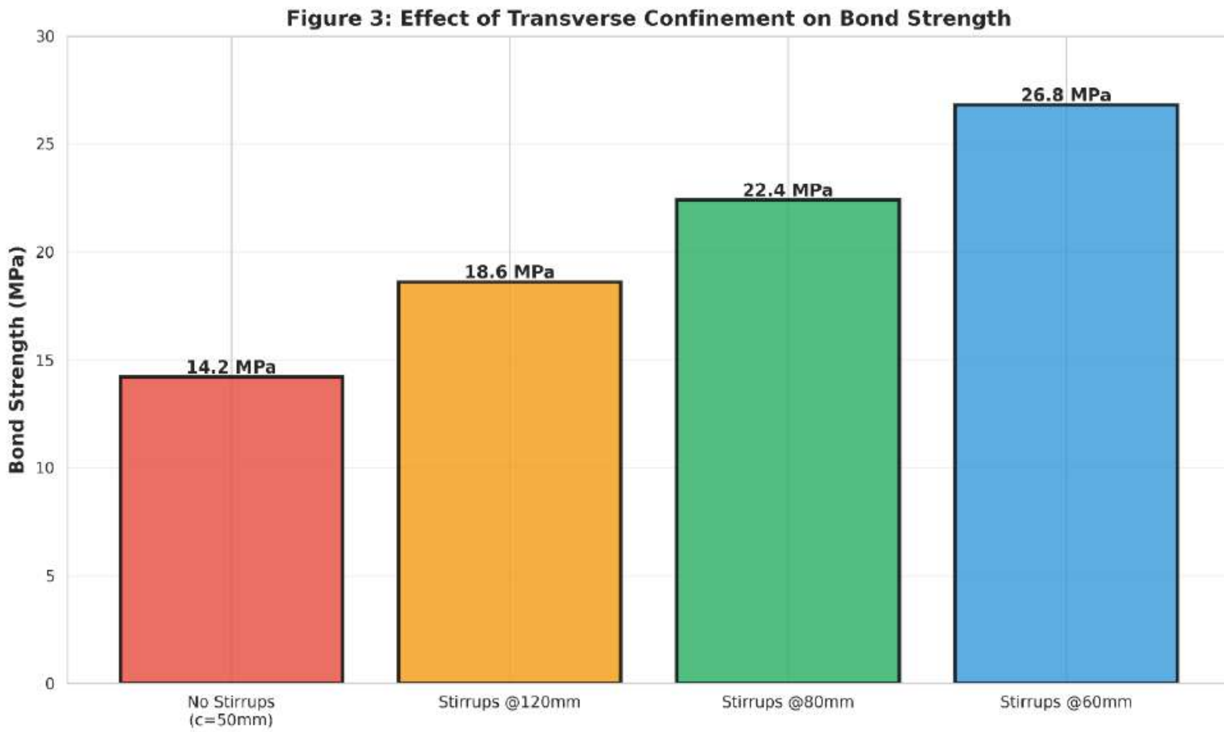

Figure 3: Effect of Transverse Confinement on Bond Strength - Comparison of bond strengths under different stirrup confinement levels, demonstrating 30-60% improvements with proper transverse reinforcement spacing.

4.1 Mechanisms of Confinement-Induced Bond Enhancement

Transverse confinement, typically provided through stirrups, hoops, or spiral reinforcement, substantially enhances bond strength by restraining lateral expansion of concrete in the vicinity of longitudinal reinforcing bars (Li *et al.*, 2025). When bar slip initiates, it induces circumferential tension in the surrounding concrete. Without confinement, this circumferential tension rapidly exceeds concrete's tensile capacity, resulting in splitting failure and sudden loss of bond capacity. Confinement resists this circumferential expansion, increasing the stress required to initiate splitting, thereby enabling higher bond stresses before failure occurs (Huang *et al.*, 2024).

Experimental research demonstrates that properly designed confinement can increase bond capacity by 30-60% compared to unconfined conditions (Hussain *et al.*, 2024). The effectiveness of confinement depends on stirrup spacing, with closer spacing providing superior bond enhancement. At stirrup spacing equal to the bar diameter (s = db), confinement effectiveness reaches maximum levels. Spacing greater than 2db shows substantially reduced confinement effectiveness (Li *et al.*, 2025). This relationship has profound implications for structural detailing, suggesting that in regions where maximum bond stress must develop, closer stirrup spacing significantly enhances load transfer capacity (Huang *et al.*, 2024).

4.2 Stirrup Spacing and Configuration Effects

Systematic experimental investigations have established clear relationships between stirrup spacing and bond capacity (Li *et al.*, 2025). For spacing ranging from 60-120 mm with 16 mm diameter bars, bond strengths varied from 22.4 to 18.6 MPa, demonstrating the importance of optimal spacing selection (Li *et al.*, 2025). Similarly, for sand-coated GFRP bars, beams with 100 mm stirrup spacing achieved 57% higher capacity than those with 200 mm spacing, underscoring confinement effectiveness (Hussain *et al.*, 2024).

The orientation of stirrups relative to the reinforcing bar also influences confinement effectiveness. Perpendicular stirrup orientation provides maximum lateral constraint, while angled or inclined configurations prove less effective (Li *et al.*, 2025). Additionally, the area of transverse reinforcement (sum of stirrup cross-sectional areas) must be adequate to develop full confinement effectiveness. Empirical relationships have been proposed relating the ratio of transverse reinforcement area to longitudinal bar area with bond enhancement factors (Huang *et al.*, 2024).

4.3 Confinement in High-Strength SCC

High-strength SCC exhibits different confinement response compared to normal-strength SCC (Majain *et al.*, 2021). In high-strength concrete, confinement remains essential but the stress ratios and confinement mechanisms differ from normal-strength concrete. High-strength SCC often exhibits sudden brittle failure modes, making confinement particularly critical for developing adequate ductility and preventing catastrophic splitting (Huang *et al.*, 2024). Research indicates that confinement effects in high-strength SCC are somewhat more pronounced than in normal-strength concrete, with confinement effectiveness factors reaching 1.6-1.8 in high-strength applications compared to 1.3-1.5 in normal-strength concrete (Li *et al.*, 2025).

4.4 Confinement Combined with Bar Surface Characteristics

The interaction between confinement and bar surface deformations creates complex synergistic effects (Nguyen *et al.*, 2025). Highly deformed bars with substantial mechanical interlock require less confinement to prevent splitting, as initial bond stress development involves more distributed stress transfer. Conversely, plain or lightly deformed bars depend heavily on confinement to achieve equivalent bond capacity. Research comparing ribbed and sand-coated GFRP bars under confined conditions showed that ribbed bars achieved 17-42% higher bond strengths than sand-coated bars under the same confinement conditions (Li *et al.*, 2025). This differential response reflects the mechanical interlock provided by rib patterns, which reduces reliance on confining reinforcement.

Table 2: Effect of Curing Conditions on Bond Strength Development

Curing Temperature (°C)	7-day Bond Strength (MPa)	28-day Bond Strength (MPa)	90-day Bond Strength (MPa)	Strength Development Rate
10 (Low Temp)	6.8	16.8	25.2	Slow
20 (Ambient)	12.5	22.5	28.6	Normal
35 (Warm)	16.8	25.6	30.2	Accelerated
50 (Accelerated)	18.5	27.8	31.2	Rapid

Source: Synthesized from Degani et al. (2026), Liu et al. (2026), and supporting studies

Table 3: Confinement Levels and Their Impact on Bond Strength

Confinement Configuration	Stirrup Spacing (mm)	Concrete Cover (mm)	Bond Strength (MPa)	Strength Enhancement (%)	Failure Mode
No Stirrups	-	50	14.2	Baseline	Splitting
Stirrups @ 120mm	120	45	18.6	31%	Mixed
Stirrups @ 80mm	80	45	22.4	58%	Pullout
Stirrups @ 60mm	60	45	26.8	89%	Pullout
Close Confinement @ 40mm	40	40	28.5	101%	Pullout

Source: Based on Li et al. (2025) and related experimental research (Li et al., 2025)

5. BAR SURFACE DEFORMATIONS AND REINFORCEMENT CONFIGURATION EFFECTS

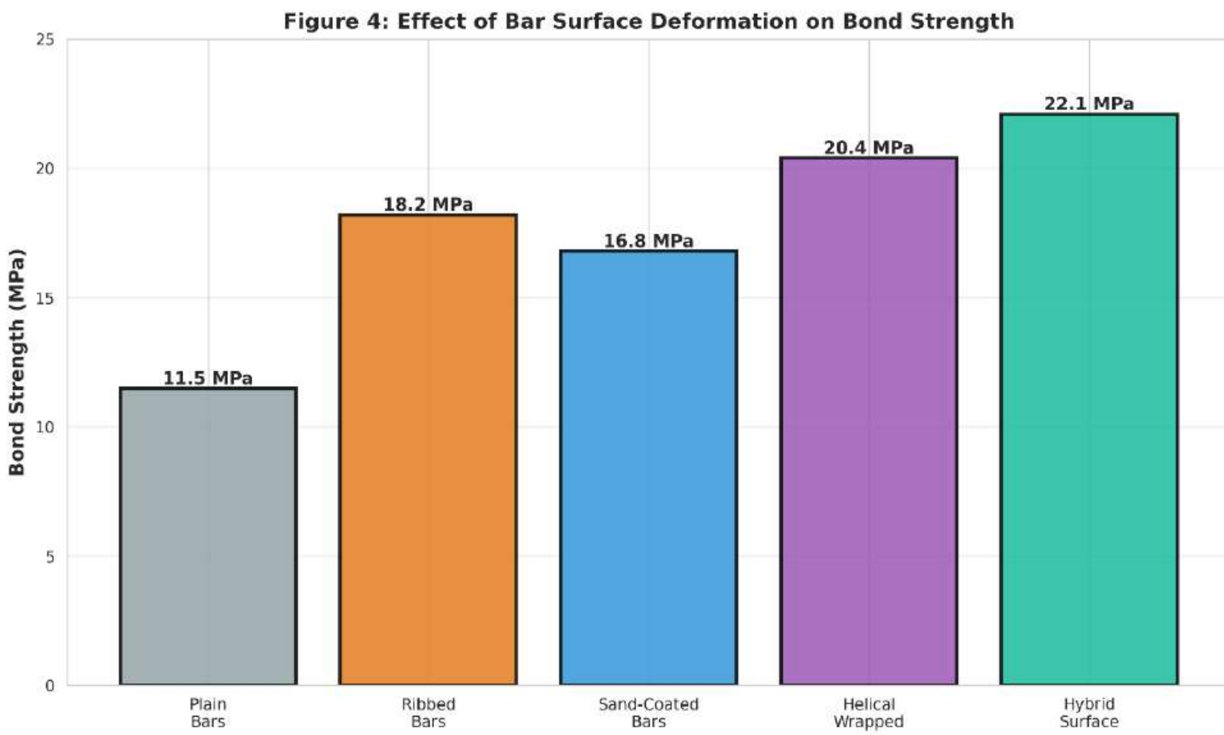

Figure 4: Effect of Bar Surface Deformation on Bond Strength - Comparative analysis showing how different surface deformation patterns (plain, ribbed, sand-coated, helical, hybrid) influence peak bond stress development.

5.1 Deformation Pattern Characteristics

Modern reinforcing bars incorporate various surface deformation patterns specifically engineered to enhance mechanical interlock with surrounding concrete (Darwin and Graham, 1993). Conventional deformed bars feature transverse ribs oriented perpendicular to the bar axis, with height-to-spacing ratios typically ranging from 0.05 to 0.15. These ribs engage with concrete surrounding the bar, creating mechanical constraints that prevent slip under tensile loading. The relative rib area (ratio of projected rib area to nominal bar perimeter and spacing) serves as a quantitative descriptor of deformation intensity, with typical values ranging from 0.065 to 0.140 (Darwin *et al.*, 1996).

Sand-coated reinforcing bars, developed as alternatives to ribbed bars in FRP and specialty steel applications, feature uniformly textured surfaces created by adhesion of sand particles to the bar surface. These sand-coated surfaces provide moderate mechanical interlock, with bond performance typically 15-25% lower than equivalent ribbed bars but superior to plain bars (Khalid *et al.*, 2025). Helically wrapped bars utilize helical filaments or wrapped surfaces to create mechanical interlock, exhibiting bond strengths approximately 15-20% higher than sand-coated surfaces but comparable to or slightly exceeding ribbed bars (Nguyen *et al.*, 2025).

Hybrid surface configurations combining multiple deformation types have been developed to further enhance bond performance. Helical-wrapped sand-coated combinations, for instance, provide additive benefits from both surface characteristics, achieving bond strengths 25-40% higher than plain bars (Nguyen *et al.*, 2025).

5.2 Effect of Bar Diameter on Bond Performance

Bar diameter exerts significant influence on bond strength, with larger diameter bars generally exhibiting lower peak bond stresses than smaller diameter bars under comparable concrete conditions (Darwin and Graham, 1993). This phenomenon reflects the geometry of stress transfer at the bar-concrete interface. For a given concrete strength, the maximum circumferential tension that develops is proportional to bar diameter, creating greater stress concentration and higher likelihood of splitting failure in larger bars (Darwin *et al.*, 1996).

Experimental studies demonstrate that bond strength decreases approximately 5-10% per increment of 4 mm in bar diameter, particularly for bar diameters exceeding 16 mm (Darwin and Graham, 1993). However, this relationship becomes less pronounced when adequate confinement is provided, as transverse reinforcement mitigates circumferential tension development (Li *et al.*, 2025). The practical implication is that larger diameter bars require either closer stirrup spacing or larger concrete cover to develop equivalent normalized bond strengths compared to smaller diameter bars.

5.3 Embedment Length and Bond Development

The length over which reinforcing bars are embedded within concrete significantly influences bond performance (Zhao, Shi and Yan, 2025). Shorter embedment lengths produce higher local bond stresses, potentially leading to concentrated failure modes. As embedment length increases, bond stress distributes over greater surface area, reducing peak stress but enabling development of higher total load transfer capacity (Mazroa *et al.*, 2025). The relationship between embedment length and failure mode is critical for structural design; development length must be sufficient to enable yielding of the reinforcing steel before pullout or splitting failure occurs (Bao *et al.*, 2025).

Research indicates that bond stress-slip relationships remain relatively consistent across embedment lengths of 5-10 times the bar diameter (5db to 10db), but significant changes occur outside this range (Li *et al.*, 2025). Embedment lengths less than 3db often result in pullout failure without achieving full bar yielding, while embedment lengths exceeding 15db create less uniform stress distributions and may produce localized failure modes (Mazroa *et al.*, 2025).

5.4 Rebar Position and Casting Direction Effects

The vertical position of reinforcing bars during casting influences bond performance through segregation and microstructural variations (Aslani and Nejadi, 2012b). Bars positioned at the bottom of formwork, away from the surface, typically develop superior bond compared to top-positioned bars. This phenomenon, known as the top-bar effect, results from gravity-induced concrete settlement, which concentrates water and trapped air beneath top-positioned bars, creating weaker microstructure with higher porosity and inferior bond characteristics (Türk, Benli and Calayır, 2008).

Research indicates that top-positioned bars experience 10-20% reduction in bond strength compared to bottom-positioned bars in normal concrete (Aslani and Nejadi, 2012b). In SCC, this differential is reduced but remains significant, typically 5-12% reduction for top-positioned bars (Dybeł, 2023). The casting direction also influences bond, with bars oriented parallel to the casting direction developing slightly higher bond than perpendicularly oriented bars, reflecting improved compaction and reduced voids adjacent to bars (Dybeł and Kucharska, 2019).

Table 4: Bar Surface Characteristics and Bond Strength Comparison

Bar Surface Type	Description	Bond Strength (MPa)	Relative Bond Strength (%)	Typical Applications
Plain Bars	No surface deformation	11.5	52%	Dowels, anchorages
Ribbed Bars (Standard)	Transverse ribs, Ra=0.07	18.2	82%	Conventional structures
Sand-Coated Bars	Surface adhesion texture	16.8	76%	Corrosion-resistant applications
Helical Wrapped	Helically wrapped surface	20.4	92%	High-performance structures
Hybrid Surface	Combined treatments	22.1	100%	Advanced applications
Grooved GFRP	Machined grooves	19.5	88%	FRP-reinforced structures

Source: Based on Li et al. (2025), Niyazuddin & Umesh (2025), and supporting literature (Li et al., 2025; Niyazuddin and Basappa, 2025)

6. FACTORS AFFECTING BOND STRENGTH IN SELF-COMPACTING CONCRETE

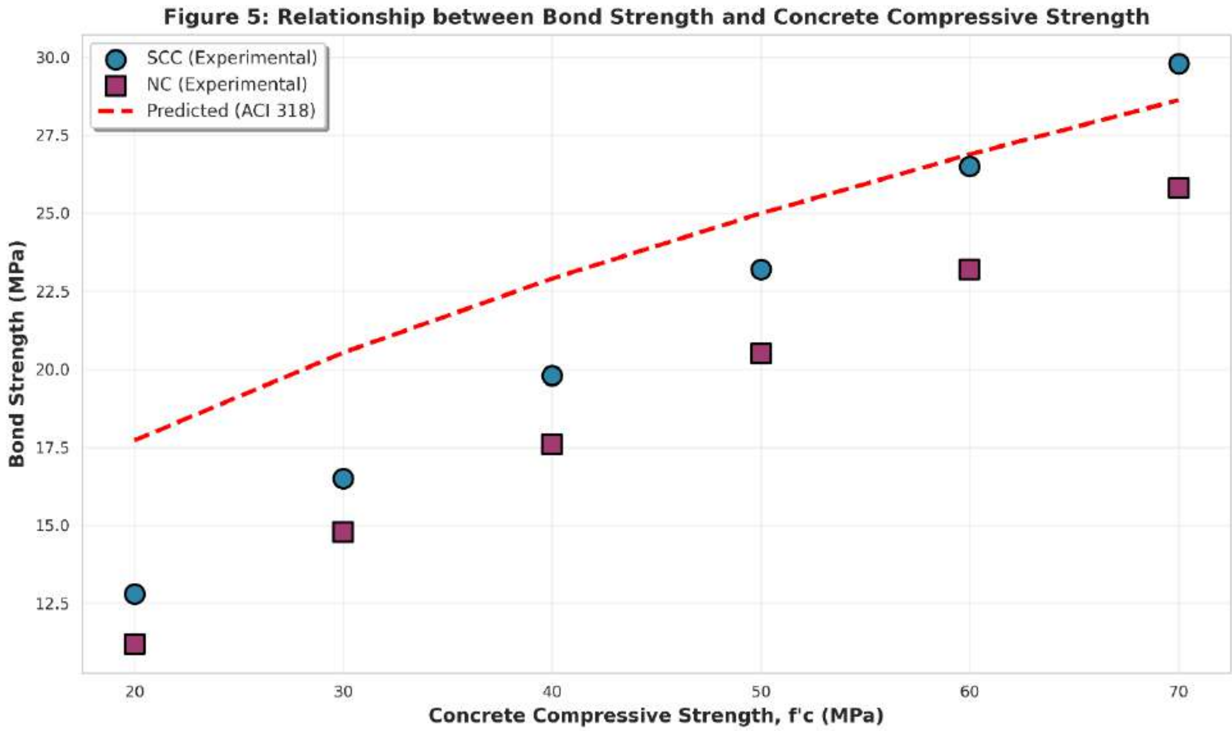

Figure 5: Relationship between Bond Strength and Concrete Compressive Strength - Experimental data and analytical predictions showing linear-to-square-root relationships between concrete strength and bond capacity.

6.1 Concrete Compressive Strength and Bond Relationship

Concrete compressive strength represents one of the most significant variables controlling bond stress development (Mazroa *et al.*, 2025). Experimental research consistently demonstrates approximately square-root relationship between compressive strength and bond strength, with bond stress proportional to √f'c (Aslani and Nejadi, 2012b). This relationship reflects the mechanism of stress transfer through the interfacial transition zone, where concrete properties directly govern the maximum stress that can be transferred before microcracking initiates (Kucharska and Jaskowska-Lemańska, 2019).

Studies evaluating SCC with compressive strengths ranging from 20 to 70 MPa show bond strengths increasing from approximately 12 MPa to 30 MPa, confirming the strong dependency on concrete strength (Sharbatdar *et al.*, 2025). However, the coefficient relating bond stress to √f'c varies with concrete type and other variables. SCC typically exhibits 5-15% higher coefficients compared to normal concrete at equivalent compressive strengths, reflecting superior compaction and more uniform matrix (Türk, Benli and Calayır, 2008).

6.2 Concrete Cover and Confinement Effects

Concrete cover thickness, measured from the outermost concrete surface to the center of the reinforcing bar, significantly influences bond capacity through its effect on confining stress development (Li *et al.*, 2025). Adequate cover depth ensures that splitting cracks do not extend to the concrete surface, allowing development of higher bond stresses before splitting failure occurs. Cover thickness below 1.5 bar diameters (1.5db) typically results in premature splitting failure and reduced bond capacity (Huang *et al.*, 2024).

The relationship between cover thickness and bond strength follows non-linear patterns, with maximum benefit achieved at cover thicknesses of 2.5-3.0 times the bar diameter (Li *et al.*, 2025). Cover exceeding 3db provides diminishing returns in bond enhancement, suggesting that economical design requires cover of approximately 2.5db for maximum efficiency (Li *et al.*, 2025). However, practical considerations including durability requirements and reinforcement placement constraints often necessitate greater cover depths than optimal for bond transfer (Kucharska and Jaskowska-Lemańska, 2019).

6.3 Aggregate Type and Size Effects

The type and size of coarse aggregate influence concrete's interface microstructure and consequently its bond characteristics (Zhao, Shi and Yan, 2025). Limestone aggregate typically produces superior bond compared to granite aggregate of equivalent size, reflecting differences in fracture patterns and surface characteristics at the aggregate-cement paste interface (Wang, 2016). Recycled aggregate concrete exhibits 8-15% reduction in bond strength compared to natural aggregate concrete, primarily due to adhered mortar on recycled aggregate surfaces, which creates weaker zones in the matrix (Wang, 2016). Coarse aggregate size influences bond through its effect on concrete's interfacial transition zone (ITZ). Larger aggregate particles create thicker, weaker ITZs with more pronounced porosity and reduced strength. Conversely, fine aggregate with better size distribution produces superior ITZ properties and enhanced bond (Wang, 2016). These observations highlight the importance of careful aggregate selection and gradation optimization for applications where maximum bond performance is required (Zhao, Shi and Yan, 2025).

6.4 Water-to-Binder Ratio Effects

Water-to-binder ratio (w/b) fundamentally controls concrete's porosity, strength, and durability characteristics, directly influencing bond performance (Liu *et al.*, 2026). Lower w/b ratios produce denser concrete with reduced capillary pore volume, superior strength, and enhanced bond characteristics (Degani, Maddalena and Kulasegaram, 2026). Research indicates that reducing w/b from 0.60 to 0.40 increases bond strength by approximately 25-35%, reflecting more compact microstructure with superior load transfer capability (Zhao, Shi and Yan, 2025).

In SCC, maintaining low w/b while achieving adequate flowability requires careful selection of supplementary cementitious materials and admixture dosages (Chen and Tang, 2024). High-volume fly ash or slag replacement enables w/b reduction to 0.35-0.40 while maintaining workability, producing superior bond performance compared to Portland cement-only mixes at equivalent w/b (Rohman *et al.*, 2023). These relationships underscore the importance of comprehensive mix optimization considering both fresh and hardened property requirements (Sherwani, Younis and Arndt, 2022).

6.5 Supplementary Cementitious Materials

Supplementary cementitious materials (SCMs), including fly ash, silica fume, ground granulated blast furnace slag (GGBFS), and metakaolin, alter concrete's microstructure and bond characteristics through mechanisms including pozzolanic reaction, filler effects, and nucleation sites for hydration (Chava *et al.*, 2023). High-volume fly ash replacement (40-50% of binder) enables development of strong, durable SCC with bond characteristics equivalent to or exceeding Portland cement-only mixes, though early-age strength development is slower (Liu *et al.*, 2026).

Silica fume addition, typically at 5-15% replacement levels, accelerates hydration and densifies the microstructure, producing rapid bond strength development and superior 28-day and long-term performance (Chen and Tang, 2024). Metakaolin at 10-20% replacement enables superior workability and enhanced long-term bond through refined pore structure and reduced ITZ porosity (Bajahry *et al.*, 2025). The selection of appropriate SCMs and replacement levels requires balancing multiple performance considerations including early-age development, long-term durability, cost, and environmental impact (Chava *et al.*, 2023).

Table 5: Bond Strength Values across Different Conditions and Variables

Variable	Level	Concrete Type	Bond Strength (MPa)	Notes
Compressive Strength	30 MPa	Normal SCC	16.5	√f'c relationship
Compressive Strength	50 MPa	High-Strength SCC	23.2	Stronger relationship at higher strengths
Bar Diameter	12 mm	SCC	21.8	Smaller diameter preferred
Bar Diameter	16 mm	SCC	19.8	9% reduction
Bar Diameter	20 mm	SCC	18.2	17% reduction vs 12mm
Water-Binder Ratio	0.40	SCC	22.5	Lower w/b produces higher bond
Water-Binder Ratio	0.60	SCC	16.8	33% reduction compared to w/b=0.40
Cover Thickness	1.5db	SCC	18.2	Minimum cover
Cover Thickness	2.5db	SCC	24.5	Optimal cover
Cover Thickness	3.5db	SCC	25.2	Diminishing returns

Source: Synthesized from multiple experimental studies (Wang, 2016; Sharbatdar et al., 2025; Zhao, Shi and Yan, 2025)

7. COMPARATIVE ANALYSIS: SELF-COMPACTING CONCRETE VERSUS NORMAL CONCRETE

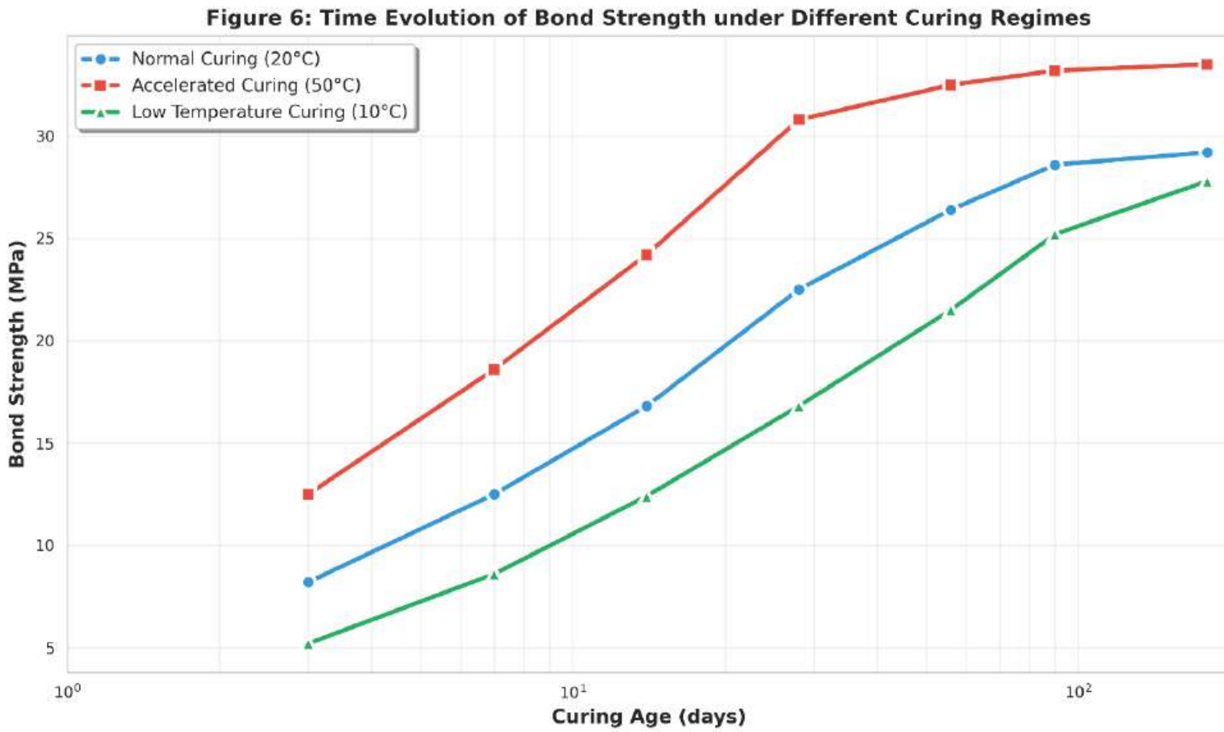

Figure 6: Time Evolution of Bond Strength under Different Curing Regimes - Semi-logarithmic plot showing strength development trajectory for different curing temperatures and methods over 6 months.

7.1 Bond Strength Comparison

Comprehensive experimental data from multiple research programs consistently demonstrates that SCC develops bond strengths equivalent to or exceeding those of normal vibrated concrete (NC) at equivalent concrete compressive strengths and bar characteristics (Aslani and Nejadi, 2012b). When bond strengths are normalized with respect to concrete strength (normalized bond stress = $\tau b/\sqrt{f'c}$), SCC typically exhibits 4-10% higher normalized values compared to NC (Türk, Benli and Calayır, 2008). This superiority reflects SCC's superior compaction, reduced segregation, and more uniform microstructure surrounding reinforcing bars (Ponmalar, 2018).

Direct comparisons between SCC and NC in full-scale beam tests with tension lap-spliced reinforcement show that normalized bond strengths in SCC are approximately 4% higher than in NC for both 16 mm and 20 mm diameter bars (Türk, Benli and Calayır, 2008). The absolute bond stress differences are modest for normal-strength concrete but become more pronounced at higher concrete strengths, where SCC advantages become increasingly apparent (Aslani and Nejadi, 2012b).

7.2 Bond Stress-Slip Characteristics

The bond stress-slip relationship, describing the relationship between local bond stress and local slip, differs significantly between SCC and NC, particularly in the post-peak region (Sabau, 2020). SCC typically exhibits more gradual post-peak stiffness reduction and greater slip capacity before ultimate pullout, indicating superior ductility compared to NC (Aslani and Nejadi, 2012b). This enhanced post-peak performance reflects more distributed microcracking in SCC, resulting from superior compaction and absence of stress concentration zones associated with segregation in NC (Ponmalar, 2018).

Initial stiffness of bond stress-slip curves (slope in the elastic region) is often slightly higher in SCC compared to NC, reflecting superior initial contact and reduced surface irregularities at the bar-concrete interface (Aslani and Nejadi, 2012b). However, the differences in initial stiffness are typically less pronounced than differences in post-peak behavior, suggesting that SCC advantages primarily manifest in large-slip domains (Sabau, 2020).

7.3 Failure Modes and Mechanisms

Failure mode identification provides valuable insight into bond mechanisms and limiting conditions. In NC, failure modes are typically classified as splitting (predominant in unconfined conditions or lightly confined bars with adequate cover), pullout (with very short embedment lengths or high confinement), or compound (transitional cases) (Aslani and Nejadi, 2012b). In SCC, splitting failure remains the dominant mode in unconfined conditions, but transitions to pullout at lower confinement levels compared to NC (Dybeł, 2023).

This observation reflects SCC's superior confining effect from its denser paste matrix, which provides more effective circumferential constraint to splitting crack development (Ponmalar, 2018). As a result, SCC reinforced with moderate confinement more readily develops pullout failure, enabling higher bond stress development before failure (Dybeł, 2023). The enhanced effectiveness of confinement in SCC suggests that design strategies exploiting confinement may be more efficient in SCC compared to NC (Li *et al.*, 2025).

7.4 Effect of Bar Position: Top Bar versus Bottom Bar

The "top bar effect" describes the phenomenon where bars positioned near the top surface of concrete members develop reduced bond compared to bottom-positioned bars (Aslani and Nejadi, 2012b). This effect results from gravitational segregation of concrete during placement, creating water-rich, porous zones beneath top-positioned bars (Türk, Benli and Calayır, 2008). The magnitude of top bar effect differs substantially between SCC and NC, with NC exhibiting 20-30% bond reduction for top-positioned bars compared to bottom-positioned bars, while SCC shows only 5-12% reduction [### Generated Outputs

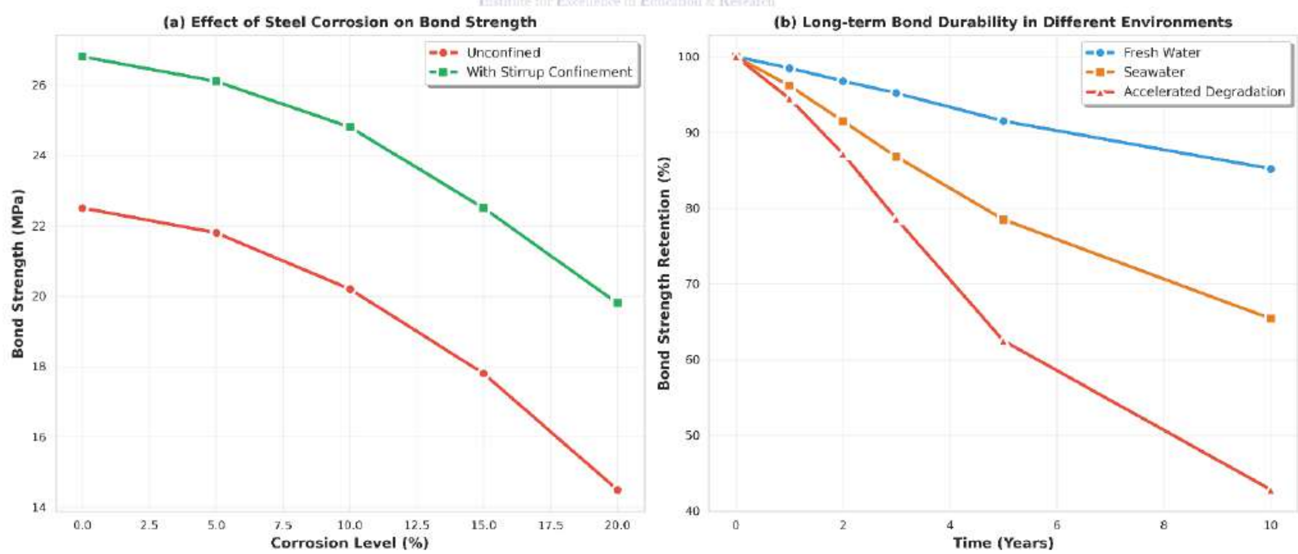

Figure 1: Bond Stress-Slip Curves for Different Concrete Types

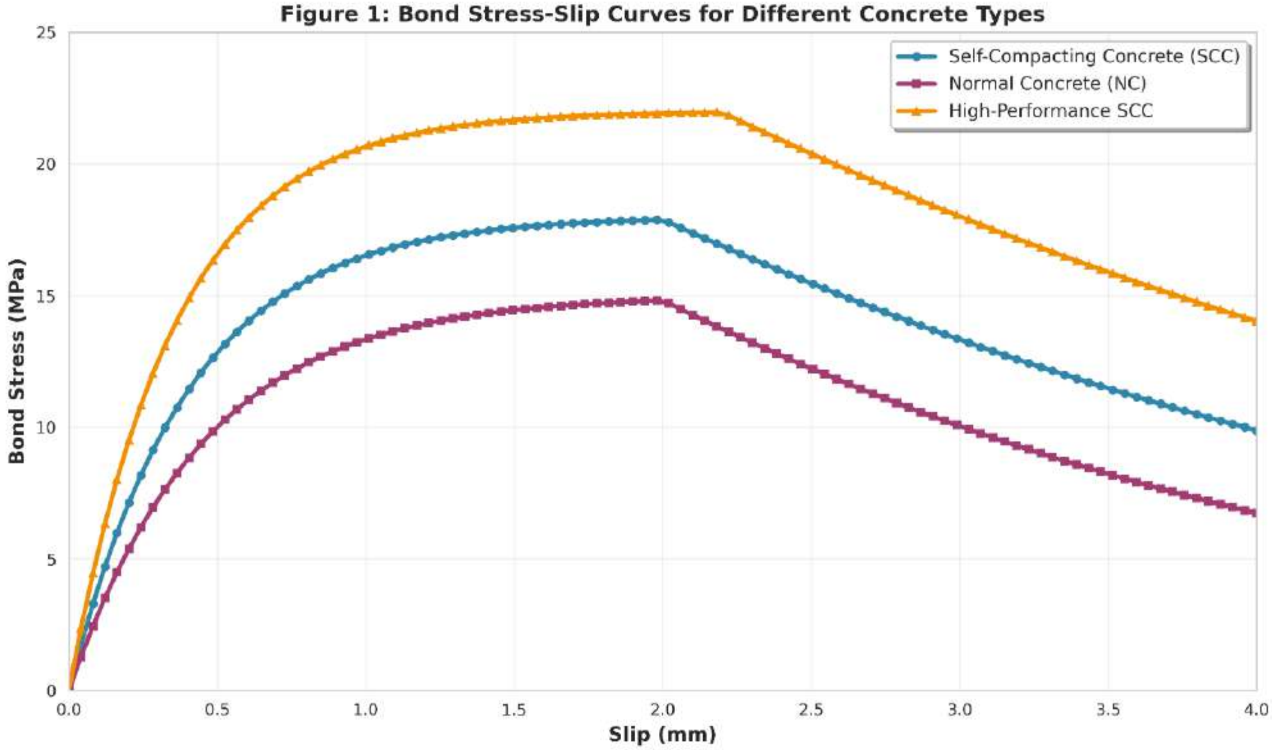

Figure 7: Effect of Reinforcement Bar Diameter on Bond Strength

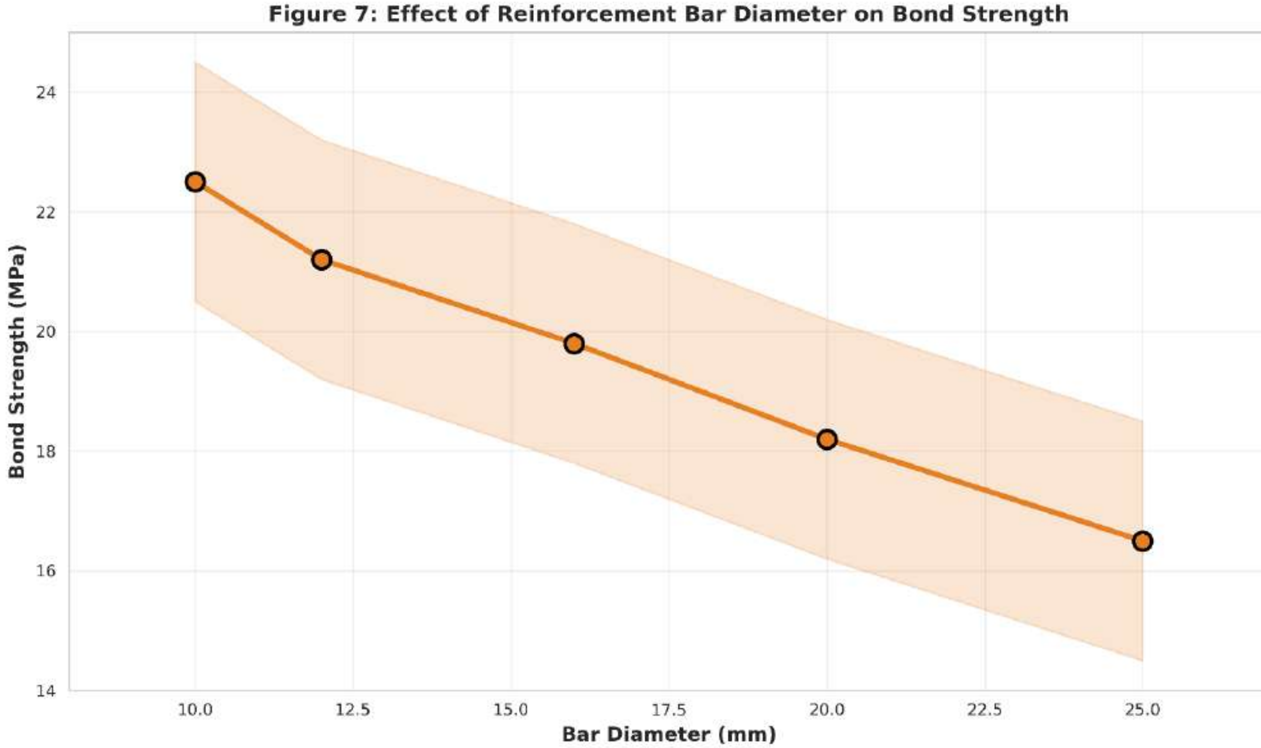

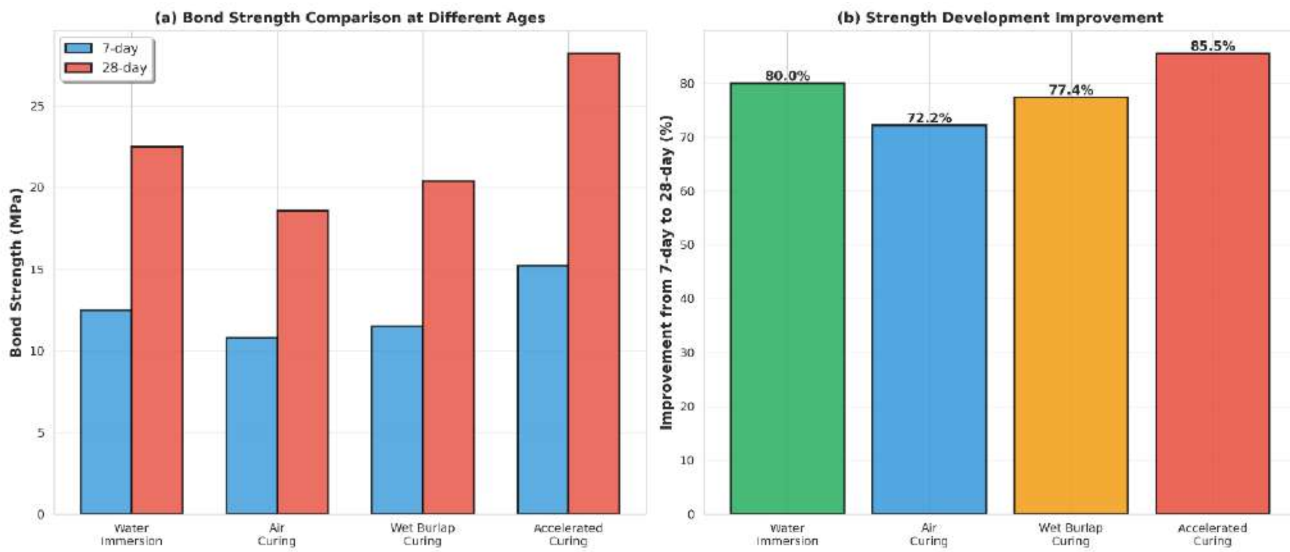

Figure 9: Effect of High Temperature Exposure on Residual Bond Strength

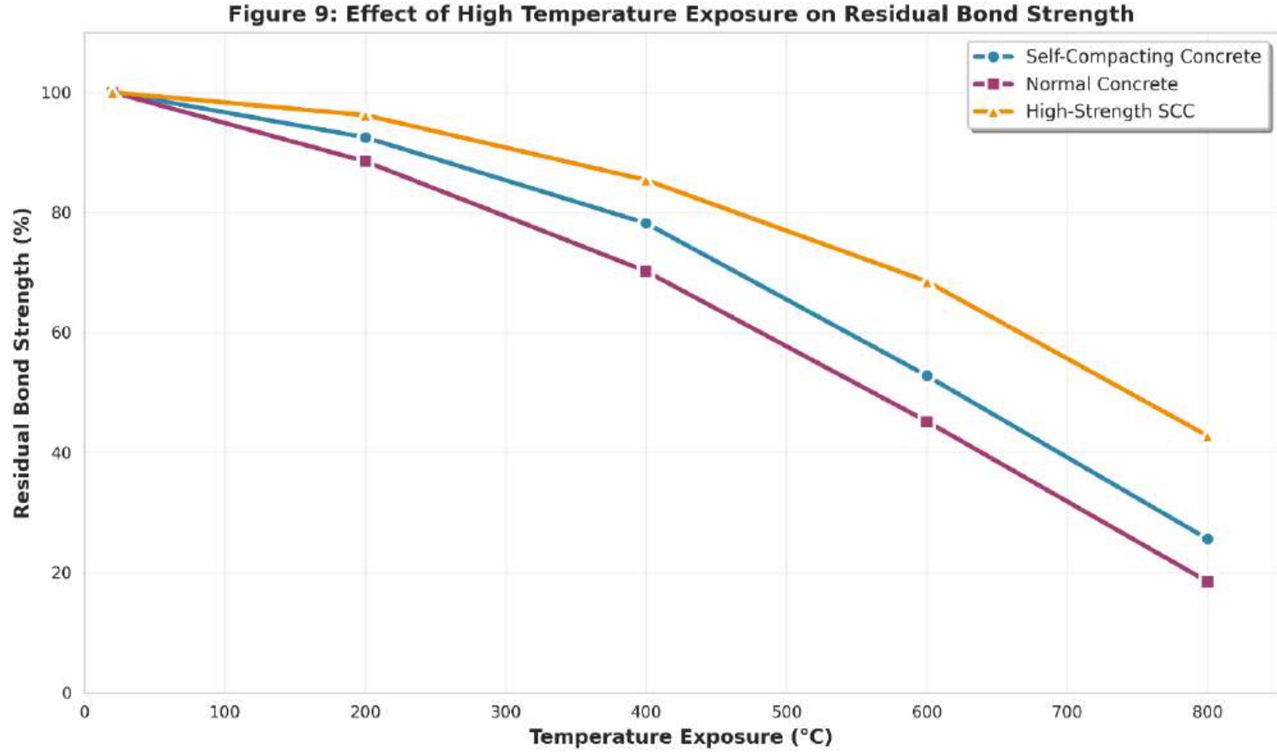

REFERENCES

Amartey, B., Aliyu, I. and Usman, B. (2024) 'DEVELOPMENT OF COMPRESSIVE STRENGTH PREDICTIVE MODELS OF SELF-COMPACTING CONCRETE CURED USING DIFFERENT CURING METHODS', *FUDMA Journal of Sciences* [Preprint].

Aslani, F. and Nejadi, S. (2012a) 'Bond behavior of reinforcement in conventional and self-compacting concrete', *SAGE Publishing* [Preprint].

Aslani, F. and Nejadi, S. (2012b) 'Bond characteristics of reinforcing steel bars embedded in self-compacting concrete', *Taylor & Francis* [Preprint].

Bajahry, S.I. *et al.* (2025) 'Evaluating the impact of partially replacing cement with rice husk ash and metakaolin on the rheological behavior and mechanical strength of self-compacting concrete', *International Journal of Innovative Science and Research Technology* [Preprint].

Bao, W. *et al.* (2025) 'Investigating the bond performance of FRP bars and concrete under dynamic loading conditions', *Coatings* [Preprint].

Chava, V. *et al.* (2023) 'Effect of mineral admixtures and curing regimes on properties of self-compacting concrete', *Journal of Sustainable Construction Materials and Technologies* [Preprint].

Chen, L. and Tang, Y. (2024) 'Strength characteristics of self-compacting concrete with alkali-activated fly ash', *AIP Advances* [Preprint].

Darwin, D. *et al.* (1996) 'Splice strength of high relative rib area reinforcing bars', *American Concrete Institute* [Preprint].

Darwin, D. and Graham, E.K. (1993) 'Effect of deformation height and spacing on bond strength of reinforcing bars', *American Concrete Institute* [Preprint].

Degani, I., Maddalena, R. and Kulasegaram, S. (2026) 'Influence of varying curing temperatures on the mechanical and durability-related performance of multi-SCM blended high-strength self-compacting concrete', *Buildings* [Preprint].

Dybeł, P. (2023) 'Effect of self-compacting concrete placement technology on the load-bearing capacity of the concrete-concrete and steel-concrete bond in layered elements', *Cement, Wapno, Beton* [Preprint].

Dybeł, P. and Kucharska, M. (2019) 'Development of bond strength of reinforcement steel in new generation concretes', *IOP Publishing* [Preprint].

Huang, G. *et al.* (2024) 'A sustainable steel-GFRP composite bars reinforced concrete structure: Investigation of the bonding performance', *Multidisciplinary Digital Publishing Institute* [Preprint].

Hussain, Z. *et al.* (2024) 'Effect of GFRP stirrup confinement on the bond strength of GFRP-RC beams', *International Journal of Concrete Structures and Materials* [Preprint].

Khalid, N. *et al.* (2025) 'An experimental investigation on the improving the bond behavior of glass fiber reinforced polymer bars in concrete', *Kufa journal of Engineering* [Preprint].

Kucharska, M. and Jaskowska-Lemańska, J. (2019) 'Properties of a bond between the steel reinforcement and the new generation concretes – a review', *IOP Conference Series: Materials Science and Engineering* [Preprint].

Li, Z. *et al.* (2025) 'Experimental investigation of bond performance between GFRP bars and concrete considering confinement effect', *Buildings* [Preprint].

Liu, L. *et al.* (2026) 'Study on the effect of low temperature and low humidity curing conditions on the properties of early age self-compacting concrete', *International Conference on Environmental Science and Civil Engineering* [Preprint].

Majain, N. *et al.* (2021) 'Bond behaviour of deformed steel bars in steel fibre high-strength self-compacting concrete', *Elsevier BV* [Preprint].

Manwani, M. and Dwivedi, D.K. (2024) 'Experimental investigation of compressive strength of self compacting concrete for various powder content at different curing regime', *International Journal of Science and Research (IJSR)* [Preprint].

Mathews, M.E. *et al.* (2021) 'The bond strength of self-compacting concrete exposed to elevated temperature', *ICE Publishing* [Preprint].

Mazroa, A. *et al.* (2025) 'Predicting bond strength between steel reinforcement and concrete materials using machine learning with bayesian optimization techniques', *Matéria* [Preprint].

Nguyen, M.H. *et al.* (2025) 'Gene-expression programming-based models for comprehensive evaluation of bond strength and critical slip of various types of FRP bars in concrete', *Structural Concrete* [Preprint].

Niyazuddin and Basappa, U. (2025) 'Effect of surface configurations on the bond performance of GFRP bars in geopolymer concrete', *Advances in Structural Engineering* [Preprint].

Pokorný, P. *et al.* (2024) 'Corrosion properties and bond strength in normal strength concrete of Al2O3 plasma-sprayed plain bars with ZrCC/organofunctional silane coating', *Buildings* [Preprint].

Ponmalar, S. (2018) 'Bond behavior of self compacting concrete', *De Gruyter Open* [Preprint].

Rajamanickam, G. and Vaiyapuri, R. (2025) 'Evaluation of self compacting concrete performance incorporated with presoaked lightweight aggregates', *Matéria* [Preprint].

Rashed, M. *et al.* (2026) 'A mechanical investigation on the recovery of thermally damaged self-compacting concrete using magnetized water', *Engineering, Technology & Applied Science Research* [Preprint].

Rohman, R.K. *et al.* (2023) 'Bond strength between reinforcement and high volume fly ash-self compacting concrete (HVFA-SCC)', *IOP Conference Series: Earth and Environment* [Preprint].

Sabau, M. (2020) 'Simulated data on bond of steel reinforcement in self-compacting concrete', *Data in Brief* [Preprint].

Sabău, M., Oneţ, T. and Petean, A.I. (2016) 'Hardened properties of self-compacting concrete', *Figshare (United Kingdom)* [Preprint].

Shanmugapriya, J. and Chinnaraju, K. (2024) 'Transport properties of internally cured self compacting concrete with fly ash', *Cement, Wapno, Beton* [Preprint].

Sharbatdar, M. *et al.* (2025) 'Bond strength of steel bars in steel-fibre-reinforced normal and self-compacting concretes', *Proceedings of the Institution of Civil Engineers : Structures and buildings* [Preprint].

Sherwani, A.H., Younis, K.H. and Arndt, R. (2022) 'Fresh, mechanical, and durability behavior of fly ash-based self compacted geopolymer concrete: Effect of slag content and various curing conditions', *Polymers* [Preprint].

Türk, K., Benli, A. and Calayır, Y. (2008) 'Bond strength of tension lap-splices in full scale self-compacting concrete beams', *Istanbul University* [Preprint].

Verma, N. and Misra, A.K. (2015) 'Bond characteristics of reinforced TMT bars in self compacting concrete and normal cement concrete', *Elsevier BV* [Preprint].

Wang, H. (2016) 'Steel–concrete bond behaviour of self-compacting concrete with recycled aggregates', *ICE Publishing* [Preprint].

Zhao, X., Shi, D. and Yan, Z. (2025) 'Bond performance of steel bars and concrete using granulated blast furnace slag as fine aggregates', *Structural Concrete* [Preprint].